ELSEVIER

Physics of the Earth and Planetary Interiors 122 (2000) 241–249

PHYSICS OF THE EARTH AND PLANETARY INTERIORS

www.elsevier.com/locate/pepi

Premonitory raise of the earthquakes' correlation range: Lesser Antilles

P. Shebalin*, I. Zaliapin, V. Keilis-Borok

International Institute of Earthquake Prediction Theory and Mathematical Geophysics, Russian Academy of Sciences, Warshavskoye sh. 79, kor. 2, Moscow 113556, Russia

Received 21 February 2000; accepted 21 August 2000

Abstract

We apply to the observed seismicity of Lesser Antilles a short term earthquake precursor which has been recently found by analysis of synthetic seismicity. The latter was generated by a lattice-type "Colliding Cascades" model of interacting elements. Precursor named *ROC* depicted premonitory increase of the earthquakes correlation range.

Here, this precursor is used as a second approximation to the intermediate-term prediction. As a first approximation we use the alarms, determined in the previous publication by the algorithm Seismic Reversal (SR); it depicts premonitory reversal of territorial distribution of seismicity.

We consider combined performance of both algorithms in prediction of earthquakes with magnitude 5.5 or above. Four such earthquakes occurred in the territory considered during 1984–1998. The alarms occupy 0.5% of the total time–space. Three alarms happened to be correct, two alarms were false and one earthquake was missed by prediction. The alarms are very stable to variation of adjustable parameters of prediction method. In view of this stability, such a prediction is unusually good even for retrospective analysis. We present this prediction method as a hypothesis to be tested on advance prediction.

Keywords: Earthquake; Prediction; Radius of correlation; Lesser Antilles

1. Introduction

Studies in earthquake prediction report many evidences that long range correlation between the earthquakes is reflected in some phenomena precursory to strong earthquakes. One of the examples is the remarkably successful prediction of the Haicheng earthquake in China, 1976 (Ma et al., 1990). On its first (long-term) stage this prediction was made by extrapolating migration of seismicity over the distances 10^3 km. Prozorov (1975, 1994) suggested that location of a future major earthquake is marked by the "distant aftershocks" — the earthquakes of medium magnitude which occur shortly after a major earthquake but on a large distances from it, far beyond the cloud of aftershocks in usual sense. In the time scale of years many premonitory seismicity patterns are formed within areas of the linear size 10 times larger than the dimension of the source of an incipient strong earthquake (Keilis-Borok, 1990; Keilis-Borok and Shebalin, 1999); this estimation is validated by advance earthquake prediction (Kossobokov et al., 1999; Vorobieva, 1990). Press and Allen (1995) have found that in the time scale tens of years this size may reach even about five times larger: earthquakes of magnitude 6 in Parkfield, CA, are preceded by the raise of seismic activity in Grand Basins and/or Gulf of Cali-

* Corresponding author. Tel.: +7-95-3107032.
E-mail address: shebalin@mitp.ru (P. Shebalin).

0031-9201/00/$ – see front matter © 2000 Elsevier Science B.V. All rights reserved.
PII: S0031-9201(00)00180-1

fornia. Such a large distances over which seismicity is correlated were well explained by microfluctuations in the movement of tectonic plates (Press and Allen, 1995) or by interaction of the crustal blocks (Soloviev and Vorobieva, 1999; Sobolev and Rundquist, 1999; Gabrielov et al., 1996). Different models explaining long-range interaction between earthquakes are naturally divided into two classes: models, rooted in statistical physics, such as renormalization models originated by Allègre et al. (1982) and Narkunskaya and Shnirman (1990), and models, based on specific local mechanisms (Gasperini and Mulargia, 1989; Gomberg et al., 1997; Hill et al., 1993; Rice and Gu, 1983; Stein et al., 1992). We emphasize that these models are *not* contradictory but complementary.

A short-term precursor "ROC" depicting increase of the earthquakes' correlation range has been recently found in synthetic seismicity. The latter has been generated by a "Colliding Cascades" model (Gabrielov et al., 2000a,b) of cellular automata type, consisting of a hierarchical system of interacting elements. Here, this precursor (ROC) is for the first time applied to the real (observed) seismicity, the corresponding prediction algorithm is called by the same name. This is done for the region of Lesser Antilles, where the test of an intermediate term prediction algorithm Seismic Reversal (SR) (Shebalin and Keilis-Borok, 1999) is currently going on. This algorithm depicts premonitory reversal of territorial distribution of seismicity.

In Sections 2 and 3 we describe applications of the algorithms SR and ROC independently of each other, both for the territory of Lesser Antilles. Algorithm SR is aimed at an intermediate-term prediction, with characteristic duration of alarms several months; it is unambiguously defined in (Shebalin et al., 1996; Shebalin and Keilis-Borok, 1999), numerical parameters included. The evidences supporting its validity, an advance prediction included, are also described in these publications. We use the published results of prediction by SR (REF), in order to juxtapose them with prediction by algorithm ROC (Section 3); the latter is aimed at a short-term prediction with duration of alarms several days.

Finally, in Section 4, which is central in this study, we use ROC as a second approximation to SR. Specifically, we consider intermediate-term alarms determined by the algorithm SR. Within these alarms we determine (by ROC) the short-term alarms.

2. Algorithm "Seismic Reversal"

Below we remind the essence of the algorithm SR and the results obtained with this algorithm in Lesser Antilles.

2.1. Performance

Prediction by SR algorithm in Lesser Antilles was aimed at the earthquakes with $M > 5$. The alarms determined in (Shebalin and Keilis-Borok, 1999) are shown in the lower row of Fig. 1a. Territory 150,000 km^2 was considered. Area of an alarm comprises between 15 and 25% of this territory. The breakdown of predictions is the following.

- Four alarms ended with earthquakes of magnitude 5.5 or more.
- Five alarms were false. During two of them two earthquakes of magnitudes 5.4 and 5.3 have occurred.
- Total duration of alarms was 59 months, 35% of the time interval considered.
- The last strong earthquake, $M = 6.0$, 24 September 1996, did occur during the alarm determined in advance.

2.2. The data

For the region considered the local earthquake catalog is routinely compiled since 1979 (Bulletins sismiques, 1979–1999). The catalog (we shall call it IPGP) is about complete for magnitudes 2.5 or more. Prior to 1979 we use the catalogue of Eastern Caribbean by Shepherd et al. (1994).

To evaluate stability of our conclusions we analyzed also the data from the worldwide NEIC/PDE catalog. It comes in three consecutively complemented issues: PDE monthly — with time delay about 1.5 years; weekly — delay about 1–2 months, and QED (quick epicenter determination; without delay) (Preliminary Determination of Epicenters, 2000). For the permanently updated versions we shall use the common name PDE; for any moment a latest available source is used. In SR application we take from PDE the magnitudes of relatively strong earthquakes, $M \geq 5$, which are practically complete in the IPGP catalog.

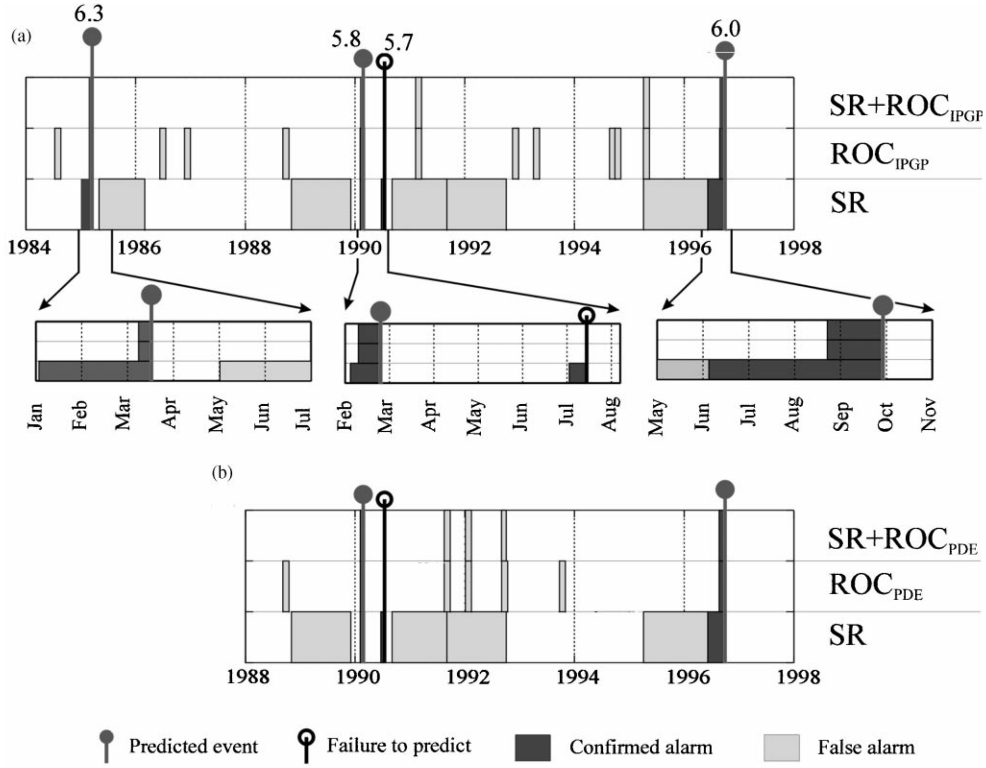

Fig. 1. Retrospective prediction, combining both algorithm SR and precursor ROC. Lower row shows alarms determined by SR; middle row: by ROC; upper row: simultaneous by SR and ROC. (a) Analysis of local earthquake catalog; 6 months around the predicted earthquakes are zoomed up. Numbers indicate the magnitude of an event. (b) Analysis of PDE catalog.

The data on magnitudes of such earthquakes are more reliable in PDE than in IPGP catalog.

The target for prediction were the earthquakes with magnitude $M \geq 5.5$. During the period considered 1984–1999 four such earthquakes have occurred, their epicenters are shown in Fig. 2. One more has occurred near the area where we applied the SR algorithm (No. 4 in Fig. 2).

2.3. The algorithm

Algorithm SR depicts premonitory reversal of territorial distribution of seismicity. According to this algorithm prior to a strong earthquake seismic activity is raising in the relatively quite areas and vice versa (Shebalin and Keilis-Borok, 1999). Its technical definition is given in all the detail in Shebalin et al. (1996).

3. Precursor "range of correlation"

This precursor depicts nearly simultaneous occurrence of two earthquakes at large distances from each other. It has been recently found in synthetic seismicity (Gabrielov et al., 2000a,b); here it is for the first time looked for in the observations.

3.1. Formal definition

As often in the study of premonitory seismicity patterns we consider a sequence of main shocks

$$\{t_k, g_k, M_k\},\ k = 1, 2, \ldots$$

Here t_k is the earthquake occurrence time, g_k the vector of the coordinates of hypocenter, M_k the magnitude, and k is the sequence number of the main shock in

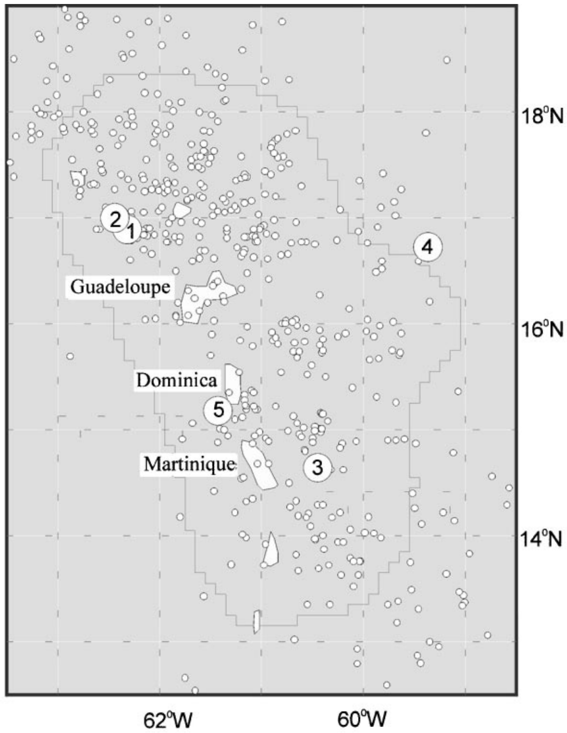

Fig. 2. Map of epicenters of earthquakes with magnitude 4 or more in Lesser Antilles. Large numbered circles: $M \geq 5.5$. Numbers correspond to the table below. Small circles-epicenters: $4 \leq M < 5.5$. The formal area where the SR algorithm can be applied is shown by the broken line

	Date	Epicenter	Depth	Magnitude
1	16 March 1985	17.01°N 62.44°W	13	6.3
2	21 February 1990	16.90°N 62.32°W	109	5.8
3	12 July 1990	14.64°N 60.45°W	28	5.7
4	8 March 1995[a]	16.67°N 59.40°W	33	6.2
5	24 September 1996	15.34°N 61.35°N	138	6.0

a. Outside the area where SR algorithm was applied..

order of the occurrence. Foreshocks are not separated from the main shocks here.

Let $R(i, j|\tau)$ be the distance between the hypocenters of two main shocks with sequence numbers i and j, $i < j$; we consider only the pairs which occurred within a narrow time interval τ, that is with $t_j - t_i \leq \tau$.

Prediction is aimed at the strong earthquakes with $M \geq M_0$. Prediction algorithm is defined as follows: an alarm is declared after a pair of earthquakes with $R \geq \Delta$. Alarm lasts for T days after second earthquake in the pair. It is called off after a strong earthquake occurs or time T expires, whichever comes first.

Additional conditions on the pairs considered: both main shocks are not too weak, with magnitude $M_{\min} \leq M < M_0$; the distance is limited from above to avoid unreasonable extensions, $R < \Delta_{\max}$.

To avoid alarms produced by a duplication of an earthquake in the catalogue we add a condition $t_j - t_i \geq 10$ min; such duplications do occur (Shebalin, 1992). In the catalogue considered this condition happened to be not necessary.

Prozorov (1975) introduced the function similar to R to identify the earthquakes of medium magnitude which occur shortly after a major earthquake but on a large distance from it. He concluded that such “distant aftershocks” mark the location of a future major earthquake.

3.2. Existence of precursor

By definition a precursor should appear more frequently, as a strong event approaches. Here, we test whether this is the case for the precursor ROC in Lesser Antilles. We use for that purpose the technique described in Fig. 3; it is developed in seismological applications of pattern recognition (Gelfand et al., 1976; Keilis-Borok and Rotwain, 1990; Press and Allen, 1995). First, we compare distribution function of R in the time intervals of two kinds: D — preceding the strong earthquakes within 6 months; and N — distanced from strong earthquakes by 6 months. The intervals are shown in Fig. 3a, the distribution functions are compared in Fig. 3b. Shift of the distribution in the intervals D toward larger values of R is clearly seen. R is determined for the main shocks with magnitudes $M \geq 3.0$ occurred within $\tau = 3$ days from each other. We cannot evaluate a statistical significance of this shift, since parameters of the functional R were not chosen a priori.

Next, we consider histograms of R (Fig. 3c) in the five bins each containing 20% of the observed values of R. This division is done for D and N intervals together; by mixing them we reduce the dangers of data fitting, since the bins do not depend on a priory knowledge on strong earthquakes (Gelfand et al., 1976). Fig. 3c shows the difference $\Delta f(R)$ between the histograms of R in D and N intervals. We see that the large values of R (starting from the

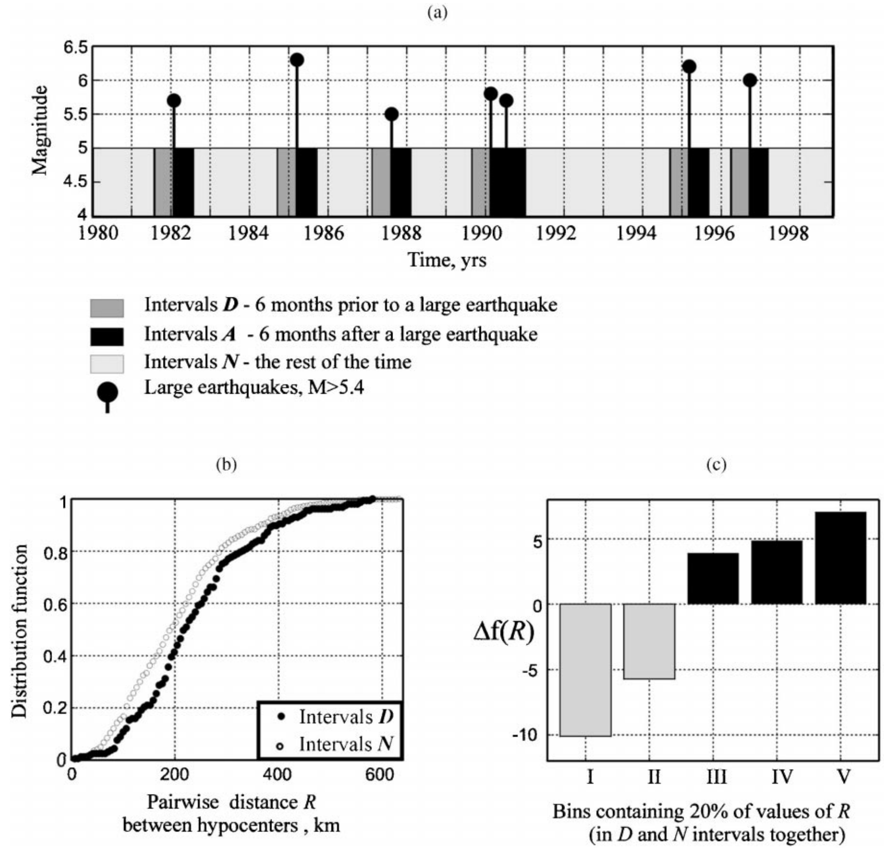

Fig. 3. Premonitory increase of the range of correlation between the earthquakes. Measure of this range is the pair-wise distance R between earthquakes' hypocenters. R is determined for the main shocks with magnitudes $M \geq 3.0$ occurred within $t = 3$ days from each other. (a) Division of the time into intervals D, A, and N. (b) Distribution functions of R in intervals D and intervals N. Shift of the distribution within the intervals D towards the large values of R is clearly seen. (c) Difference $\Delta f(R)$ of distributions of R in intervals D and N. Each bin corresponds to an interval containing 20% of all the values of R considered. Large values of R (bins III–V) are obviously concentrated within 6 months prior to a large earthquake (in the intervals D).

third bin, i.e. $R > 150$ km) are more frequent in D intervals.

3.3. Performance of the precursor

Existence of a precursor per se is not sufficient to ensure its satisfactory performance in prediction of earthquakes one by one. For example, most of precursors may be concentrated before one of strong events leaving others unpredicted. To evaluate performance of precursor ROC we apply the algorithm defined in Section 3.1 with the following numerical parameters: target of prediction is an earthquake with magnitude not lower than $M_0 = 5.5$; duration of alarm $T = 40$ days; time window $\tau = 3$ days; threshold for declaration of alarm $\Delta = 150$ km, $\Delta_{\max} = 300$ km; $M_{\min} = 3.8$.

Strong earthquakes and alarms determined by this precursor are shown in the middle row of Fig. 1a.

Altogether 13 short-term alarms are determined, three strong earthquakes happened during these alarms, one strong earthquake is missed, and 10 alarms are false. Total duration of alarms is 10% of the considered interval. This performance is not satisfactory: although total duration of alarms is low (since they are the short-term ones) the number of false alarms is too large.

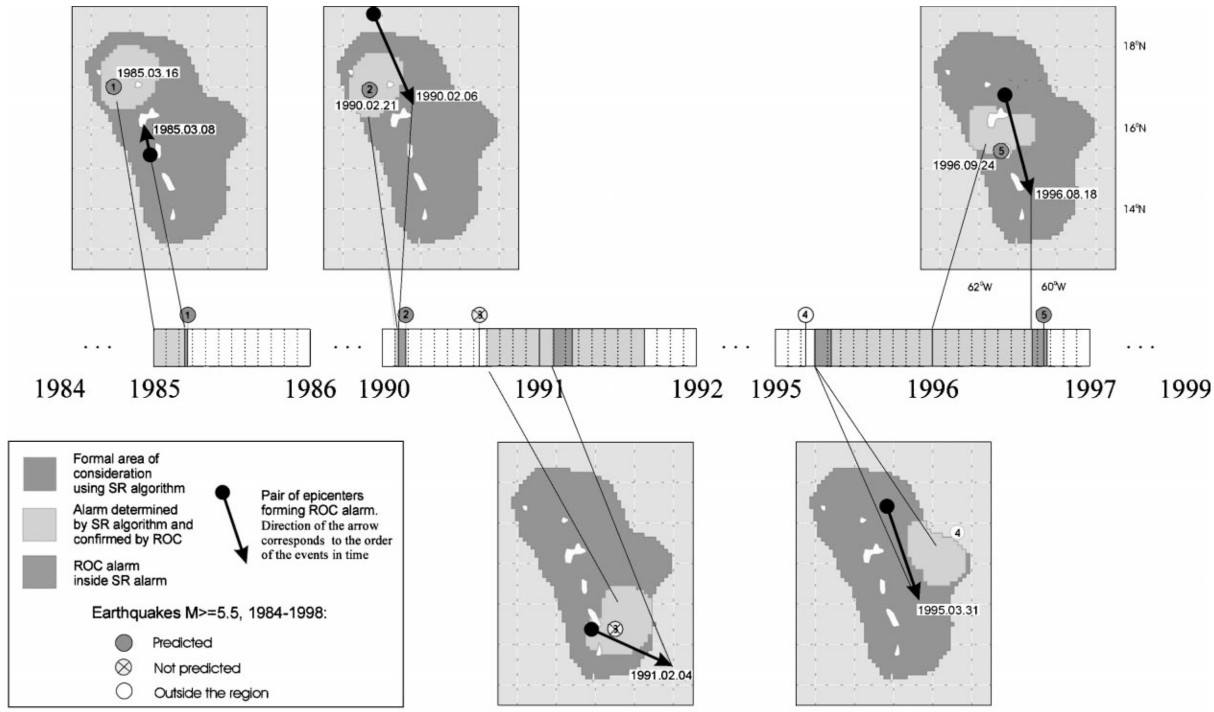

Fig. 4. Transition to short term prediction in time and space. Intervals without joint SR and ROC alarms nor strong earthquakes are lapsed on the figure. Pairs of events forming ROC precursor seem to occur in the same part of the region. False alarms determined by both SR and ROC probably were initiated by preceding strong earthquakes.

4. Consecutive application of the algorithms: transition to short-term prediction

4.1. Joint performance

Earthquake prediction research knows just a few but very successful examples of reproducible consecutive predictions with increasing accuracy. Among them is prediction of Haicheng earthquake in China, 1976, which went through four stages from long-term to immediate (Ma et al., 1990); and increase of territorial accuracy of intermediate-term prediction by the algorithm “Mendocino Scenario” (Kossobokov et al., 1990). For the latter high statistical significance is established by massive application to strongest earthquakes of Circum Pacific belt (Kossobokov et al., 1999); short-term precursors on the background of intermediate-term ones is reported also in (Kossobokov et al., 1999).

Comparison of alarms determined by SR and ROC (lower and middle rows in Fig. 1) suggests a next step: to regard ROC as a second approximation to SR and declare an alarm in two stages.

1. Intermediate term alarms are defined by algorithm SR.
2. During these alarms we define the short-term alarms by algorithm ROC.

Alarms determined in this way are shown in the top row of Fig. 1a. We see that three out of four strong earthquakes happened during a short term alarm. Two alarms are false. Total duration of alarms is 3% of time considered. Fig. 4 shows how short-term prediction by two algorithms, thus combined, was unraveled in space and time. An area of alarm occupies 15–25% of the territory, and all alarms together occupy 0.5% of the time-space considered. In advance prediction any of such scores would be

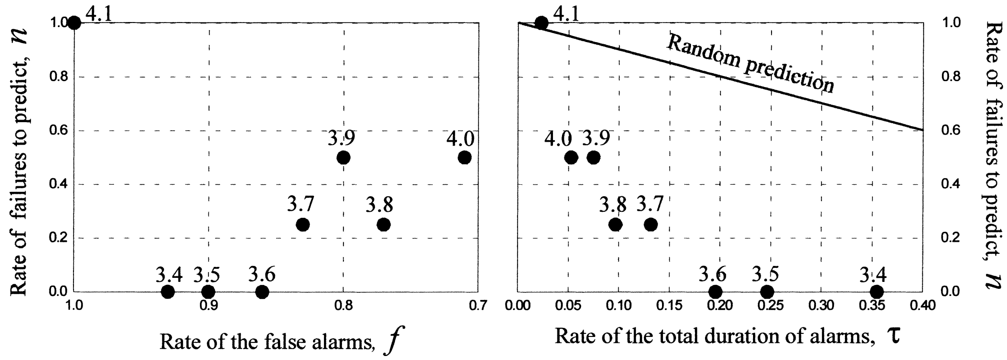

Fig. 5. Error diagrams for precursor ROC. Different points correspond to different threshold M_{min} given in the figure. Other parameters are fixed as follows: $\tau = 3$ days, $\Delta = 150$ km, $\Delta_{max} = 1000$ km, and $T = 40$ days.

a great success. Note that SR alarms have been determined for magnitude threshold $M_0 = 5$. We use these alarms here because they have been published in paper (Shebalin and Keilis-Borok, 1999) a priori. The difference in M_0 only lowers our success score, since false alarms by ROC have smaller chance to be eliminated.

Arrows on the Fig. 4 connect the first and second in the pairs of earthquakes which generated an alarm. It is interesting to note that both lie close to the area, covered by the SR alarm. The second earthquake is within 100 km from the epicenter of incipient strong earthquake, much less than the dimension of the area considered (about 150,000 km^2).

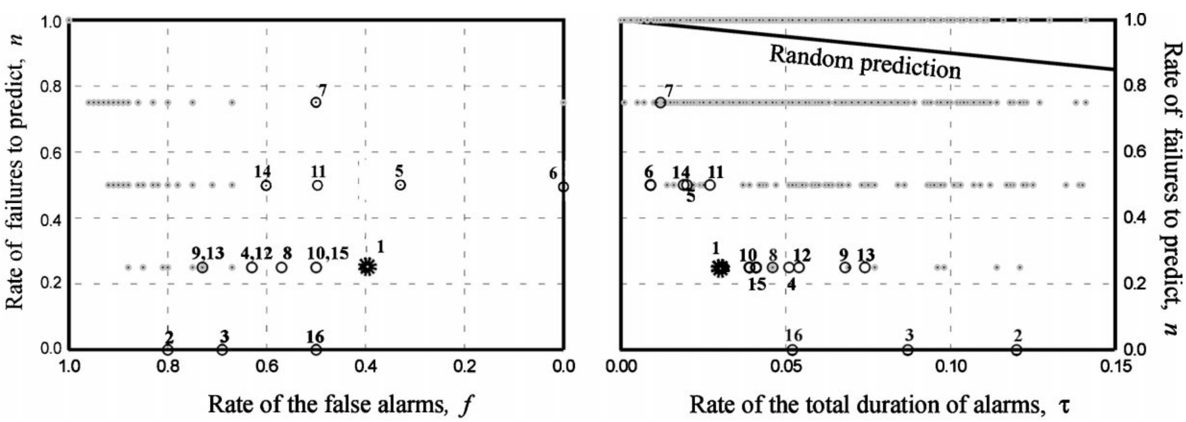

Fig. 6. Error diagrams for prediction by SR and ROC jointly. Different circles correspond to different adjustable parameters of the precursor ROC (see table below). Point no. 1 corresponds to the parameters used in the analysis illustrated in Fig. 1. Small gray circles correspond to the randomized alarms used to check significance of the result (see explanation in the text)

	1[a]	2	3	4	5	6	7	8	9	10	11	12	13	14	15
M_{min}	3.8	3.5	3.6	3.7	4.0										
τ, days	3					1		5							
Δ, km	150								50	100	200				
Δ_{max}, km	300						250					400	500		
T, days	40													20	60

[a] Values which are the same as in the first column are not indicated in the table.

4.2. Stability and non-randomness of predictions

Stability of predictions to variation of adjustable parameters of prediction algorithm is characterized by the error diagrams introduced in earthquake prediction research by Molchan (1997). The error diagram also is a tool for quantitative analysis of a prediction algorithm performance: it allows to estimate prediction algorithm strength and compare different algorithms and strategies. These diagrams are shown in Fig. 5 for ROC and in Fig. 6 for ROC and SR jointly. In both cases only parameters of the ROC are varied since we used the already published alarms by SR. Stability of results is quite acceptable: the results can hardly be improved for ROC alone, or destroyed for joint application of ROC and SR.

Fig. 6 shows also a randomized prediction. A combination of adjustable parameters (table at the bottom of Fig. 6) is randomly selected. For each combination we know the number N (4–40) of alarms and their duration T. We distribute randomly the same number of alarms, of the same duration. The scores of (n, τ) and (n, f) is shown by gray dots in Fig. 6. Obviously, the random predictions give much inferior score, just a few of them overlap with predictions by the combined algorithm considered here.

5. Conclusion

We have demonstrated a two-stage prediction: short term precursors used as a second approximation to the intermediate term alarms. This fetched short-term prediction of high quality unusual even in retrospective analysis. It is encouraging that considerable part of analysis did not involve retrospective data fitting. We used as a first approximation the intermediate-term alarms determined in a previous publication (by the algorithm SR). In a second approximation we used a new type of precursors (ROC) formally defined by analysis of synthetic seismicity; in this study it is for the first time applied to observations. One should remember, however, that adjustable parameters of this precursor could not be determined a priori on a model and were data fitted on observations considered here. Accordingly this study merely formulates a hypothesis, to be tested on independent data; the only final test is an advance prediction.

This study also supports the conclusion made in (Gabrielov et al., 2000a,b) on existence of premonitory increase of the range of correlation between the earthquakes.

Acknowledgements

This study was partly supported by the grants from the National Sciences Foundation (EAR-9804859) and the Italian Ministry for Foreign Affairs. We thank N. Girardin and J.P. Viodé for providing the Seismic Bulletin of French Stations in Antilles. We are also grateful to the anonymous reviewer for the constructive criticism.

References

Allègre, C.J., Le Mouël, J.L., Provost, A., 1982. Scaling rules in rock fracture and possible implications for earthquake prediction. Nature 297, 47–49.

Bulletins sismiques des Observatoires des Antilles, 1979–1999. Departement des Observatoires volcanologiques, Institut de Physique du Globe de Paris.

Gabrielov, A., Keilis-Borok, V.I., Jackson, D.D., 1996. Geometric incompatibility in a fault system. Proc. Natl. Acad. Sci. U.S.A. 93 (9), 3838–3842.

Gabrielov, A.M., Keilis-Borok, V.I., Zaliapin, I.V., Newman, W.I., 2000a. Critical transitions in colliding cascades. Phys. Rev. E 62, 237–249.

Gabrielov, A.M., Keilis-Borok, V.I., Zaliapin, I.V., Newman, W.I., 2000b. Colliding cascades a the model for earthquake prediction, JGI 143, in press.

Gasperini, P., Mulargia, F., 1989. A statistical analysis of seismicity in Italy: the clustering properties. BSSA 79 (4), 973–988.

Gelfand, I., Keilis-Borok, V.I., Knopoff, L., Press, F., Rantsman, E., Rotwain, I., Sadovsky, A., 1976. A pattern recognition applied to earthquake epicenters in California. Phys. Earth Planet. Inter. 11, 227–283.

Gomberg, J., Blanpied, M.L., Beeler, N.M., 1997. Transient triggering of near and distant earthquakes. BSSA 87 (2), 294–309.

Hill, D.P., Reasenberg, P.A., Michael, A., Arabasz, W.J., Beroza, G., Brumbaugh, D., Brune, J.N., Castro, R., Davis, S., dePolo, D., Ellsworth, W.L., Gomberg, J., Harmsen, S., House, L., Jackson, S.M., Johnston, M., Jones, L., Keller, R., Malone, S., Munguia, L., Nava, S., Pechmann, J.C., Sanford, A., Simpson, R.W., Smith, R.S., Stark, M., Stickney, M., Vidal, A., Walter, S., Wong, V., Zollweg, J., 1993. Seismicity remotely triggered by the magnitude 7.3 Landers, California, earthquake. Science 260, 1617–1623.

Keilis-Borok, V.I. (Ed.), 1990. Intermediate-term earthquake prediction: models, phenomenology, worldwide tests. Phys. Earth Planet. Inter. 61 (Special Issue), 1, 2, 144.

Keilis-Borok, V.I., Rotwain, I.M., 1990. Diagnosis of time of increased probability of strong earthquakes in different regions of the world: algorithm CN. Phys. Earth Planet. Inter. 61, 57–72.
Keilis-Borok, V.I., Shebalin, P.N. (Eds.), 1999. Dynamics of lithosphere and earthquake prediction. PEPI 111 (Special Issue), 179–330.
Kossobokov, V.G., Keilis-Borok, V.I., Smith, S.W., 1990. Localization of intermediate-term earthquake prediction. J. Geophys. Res. 95, 19763–19772.
Kossobokov, V.G., Romashkova, L.L., Keilis-Borok, V.I., Healy, J.H., 1999. Testing earthquake prediction algorithms: statistically significant advance prediction of the largest earthquakes in the Circum-Pacific, 1992–1997, PEPI, 111, 187–196.
Ma, Z., Fu, Z., Zhang, Y., Wang, C., Zhang, G., Liu, D., 1990. Earthquake Prediction: Nine Major Earthquakes in China. Springer, New York.
Molchan, G.M., 1997. Earthquake prediction as a decision-making problem. PAGEOPH 149, 233–247.
Narkunskaya, G.S., Shnirman, M.G., 1990. Hierarchical model of defect development and seismicity. Phys. Earth Planet. Inter. 61, 29–35.
Preliminary Determination of Epicenters (PDE): PDE monthly. FTP at the address gldfs.cr.usgs.gov/pde; PDE weekly and QED, FTP at gldfs.cr.usgs.gov/weekly.
Press, A., Allen, C., 1995. Pattern of seismic release in the southern California region. J. Geophys. Res. 100, 6421–6430.
Prozorov, A.G., 1975. Changes of seismic activity connected to large earthquakes. Interpretation of data in seismology and neotectonics. Computational Seismology, Vol. 8, Nauka, Moscow, pp. 71–82.
Prozorov, A.G., 1994. A new test for the statistical significance of distant interaction of large earthquakes. Seismisity and related processes in the environment. Global Changes of Environment and Climate, Federal Research Program of Russia, Vol. 1, Russian Academic Science, pp. 69–73.
Rice, J., Gu, J., 1983. Earthquake after effects and triggered seismic phenomena. Pageof 121, 187–219.
Shebalin, P.N., 1992. Automatic duplicate identification in set of earthquake catalogues merged together. US Geol. Surv. Open-File Report 92-401, Appendix II.
Shebalin, P., Girardin, N., Rotwain, I., Keilis-Borok, V., Dubois, J., 1996. Local overturn of active and non-active seismic zones as a precursor of large earthquakes in Lesser Antillean arc. PEPI 97, 163–175.
Shebalin, P.N., Keilis-Borok, V.I., 1999. Phenomenon of local "seismic reversal" before strong earthquakes. PEPI 111, 215–227.
Shepherd, J.B., Linch, L.L., Tanner, J.G., 1994. A revised earthquake catalogue for the Eastern Caribbean region. In: Proceedings of the Caribbean Conference on Natural Hazards, Trinidad and Tobago, 1993.
Sobolev, P.O., Rundquist, D.V., 1999. Seismicity of oceanic and continental rifts: a geodynamic approach. PEPI 111, 253–266.
Soloviev, A., Vorobieva, I, 1999. Long-range interaction between synthetic earthquakes in the model of block structure dynamics. In: Proceedings of the Fifth Workshop on Non-Linear Dynamics and Earthquake Prediction, Trieste: ICTP, H4.SMR/1150-4, 4–22 October 1999, 18 pp.
Stein, R.S., King, G.S.P., Lin, J., 1992. Change in failure stress on the Southern San-Andreas fault system caused by the 1992 (magnitude = 7.4) Landers earthquake. Science 258, 1328–1332.
Vorobieva, I.A., 1990. Prediction of a subsequent large earthquake. PEPI 111, 197–206.